Pergamon

J. Quant. Spectrosc. Radiat. Transfer Vol. 60, No. 4, pp. 531–542, 1998

Printed in Great Britain
PII: S0022-4073(97)00238-0
0022–4073/98 $19.00 + 0.00

SHIFT AND WIDTH OF HeII LINES

MICHAEL STOBBE,† AXEL KÖNIES,‡ SIBYLLE GÜNTER‡§ and JACEK HALENKA¶

†Fachbereich Physik, Universität Rostock, Universitätsplatz 1, 18051 Rostock, Germany; ‡Max-Planck-Institut für Plasmaphysik, Boltzmannstr. 2, 85748 Garching, Germany and ¶ Institute of Physics, Pedagogical University of Opole, 45-052 Opole, ul. Oleska 48, Poland

(Received 3 July 1997)

Abstract—Based on a quantum statistical many-particle theory, the shift and the width of some He II lines have been evaluated. Ion dynamics have been treated within the model microfield method. Furthermore, fine structure splitting has been taken into account in order to check whether this effect is the cause for the existing large discrepancies between theoretical and experimental line widths. Besides the electronic contributions to the line shift, the shift due to the inhomogeneities of the ionic microfield as well as that due to the quadratic Stark effect has been included. © 1998 Elsevier Science Ltd. All rights reserved.

1. INTRODUCTION

One of the most important tools for plasma diagnostics is the shape of the emitted spectral lines. Whereas for plasmas of moderate densities and temperatures hydrogen spectral lines play an important role for plasma diagnostics, in hot and dense plasmas most of the radiators are highly ionized. Therefore, for such plasma conditions which can be found, for example, in laser produced or astrophysical plasmas, the knowledge of the line shapes of highly ionized or even hydrogenic ions allows to determine the electron density or the temperature.

Up to now, there are large discrepancies between theoretical and experimental results. It has been supposed that the reasons for these discrepancies are experimental uncertainties[2] or the neglect of fine structure splitting by the theories.[1] During the last few years precise measurements of spectral line profiles of some He II lines have been carried out. That is why, the aim of this paper is to calculate the line widths for these experimental plasma parameters. Thereby, fine structure splitting will be included in order to investigate whether the agreement between theoretical and experimental results can be improved this way. Furthermore, the line shift will be evaluated. In difference to former theories it will be determined from a complete shifted and asymmetric line profile.

The starting point of our theoretical investigations is a Green's function approach to spectral line shapes which has been developed for the case of neutral radiators.[3–6] Starting from the relationship between the complex refraction index and the dielectric function, a many-particle approach to the optical properties of dense plasmas has been developed. Thereby, not only the radiators but also the perturbers have been treated quantum mechanically. Avoiding a no-quenching approximation, besides the line width also its shift has been calculated. Taking into account further the interaction between the radiator and the inhomogeneities of the ionic microfield as well as the quadratic Stark effect, the ionic contributions to the shift of the line and to its asymmetry have been included. Ion dynamics have been treated via the well-known model microfield method.[7–10]

In order to deal with charged radiators, the theoretical approach has to be modified in some points. Besides changes in the wave functions and energy values, the interaction between the radiator and the perturbers has to be reconsidered. This will be done for the electronic as well as for the ionic contributions to the line profile.

§To whom all the correspondence should be addressed.

Ion dynamics will be included via the well-known model microfield method (MMM). For that reason a field-field autocorrelation function for charged radiators will be calculated in order to determine the corresponding jumping frequency.

Dealing with the shift of spectral lines caused by the plasma ions, a generalized mean field gradient $B_p(\beta)$ has been introduced by one of the authors.[11] This treatment of the ionic contributions to shift and asymmetry has been proved already to be successful for hydrogen lines.[11,12] It will be modified here for the case of charged radiators.

2. THEORY

Based on a Green's function technique, a quantum mechanical many-particle approach to spectral line profiles has been developed.[3-6] It has been shown that the shape of spectral lines is given by the two-particle contributions to the corresponding polarization function. Therefore, the line profile emitted by a radiator that moves with the momentum $\boldsymbol{P}$ is given by

$$I(\Delta\omega) \sim \sum_{ii'ff'} I_{if}^{i'f'}(\Delta\omega) \exp\left[-\frac{P^2}{2Mk_BT}\right] \langle i|\langle f|[U(\Delta\omega)]^{-1}|f'\rangle|i'\rangle \tag{1}$$

with

$$U(\Delta\omega) = \Delta\omega - \frac{\boldsymbol{Pk}}{M} - \frac{k^2}{2M} - \mathrm{Re}\{\Sigma_i - \Sigma_f\} + \mathrm{i}\,\mathrm{Im}\{\Sigma_i + \Sigma_f\} + \mathrm{i}\Gamma^v. \tag{2}$$

M denotes here the radiator's mass, k_B is the Boltzmann constant, T the temperature of the heavy plasma particles, and k the wave number of the emitted radiation. The sum has to be carried out over all transitions which contribute to the spectral line. The intensity

$$I_{if}^{i'f'}(\Delta\omega) = M_{if}^{(0)}(\boldsymbol{k})\,[M_{i'f'}^{(0)}(\boldsymbol{k})]^*\, I(\Delta\omega) \tag{3}$$

besides the transition matrix elements contains the frequency dependence of the dipole radiation and that resulting from the Boltzmann occupation of the radiator's states. It is responsible for the so-called "trivial asymmetry".

The influence of the surrounding plasma on the radiator is contained in the self energy Σ. The real part of the self energy corresponds to the shift of the concerning energy level, whereas its imaginary part gives the width. The line shift follows from the difference of the shifts of the upper and the lower energy level. The line width, however, results from the sum of the corresponding level widths. The vertex term Γ_{if}^{v} describes the coupling of the upper and the lower energy state. In principle, it represents the interference contribution to the quantum-mechanical summation of the widths of both energy states.

For the plasma conditions which are of interest here, it is possible to decouple the ionic and the electronic subsystems of the plasma. Assuming a static ionic microfield $\boldsymbol{E}$, one finds for the self energy

$$\Sigma = \Sigma^{\mathrm{ion}}(E) + \Sigma^{\mathrm{el}}(E, \Delta\omega). \tag{4}$$

Whereas the ionic part of the self energy describes the influence of the static ionic microfield on the radiator, the electronic contribution depends on both, the ionic microfield and the detuning $\Delta\omega$ from the line center. The aim of this paper is to give the electronic as well as the ionic contributions to the self energy for a charged radiator. Considering spectral lines of hydrogenic ions, it is well known that their width is considerably smaller than that of the corresponding neutral radiators. That is why, one has to account for ion dynamics as well as for fine structure splitting. Ion dynamics will be taken into account here within the model microfield method.[7-10] Applying the often used Kangaroo-process, instead of Eq. (2) one finds

$$\begin{aligned}\langle U(\Delta\omega)\rangle_{\mathrm{KP}} = {} & \langle U(\Delta\omega|\boldsymbol{E})\rangle_s + \langle \Omega(\boldsymbol{E})\, U(\Delta\omega|\boldsymbol{E})\rangle_s [\langle \Omega(\boldsymbol{E})\rangle_s \\ & - \langle \Omega^2(E)\, U(\Delta\omega|\boldsymbol{E})\rangle_s]^{-1} \langle \Omega(E)\, U(\Delta\omega|\boldsymbol{E})\rangle_s.\end{aligned} \tag{5}$$

The time development operator for a constant ionic microfield strength $U(\Delta\omega|\boldsymbol{E})$ is given by

$$U(\Delta\omega|\boldsymbol{E}) = \Delta\omega - \frac{\boldsymbol{Pk}}{M} - \frac{k^2}{2M} - \mathrm{Re}\{\Sigma_i - \Sigma_f\} + \mathrm{i}\Omega(E) + \mathrm{i}\,\mathrm{Im}\{\Sigma_i + \Sigma_f\} + \mathrm{i}\Gamma^v. \tag{6}$$

The average $\langle \ldots \rangle_s$ has to be carried out applying the corresponding microfield distribution function $W(E)$

$$\langle \ldots \rangle_s = \int \mathrm{d}E\, W_\rho(E) \ldots . \tag{7}$$

For the case of neutral radiators, the jumping frequency $\Omega(E)$ has been determined from the field-field autocorrelation function

$$\Gamma(t) = \frac{4\pi n_e e^2}{t} \sqrt{\frac{2m}{\pi k_B T}} \left[1 + \tau^2 - \sqrt{\pi}\tau \left(\tau^2 + \frac{3}{2} \right) \mathrm{e}^{\tau^2} \mathrm{erfc}(\tau) \right], \tag{8}$$

with

$$\tau = \frac{\omega_{pl} t}{\sqrt{2}}, \tag{9}$$

$$\mathrm{erfc}(x) = \frac{2}{\sqrt{\pi}} \int_x^\infty \mathrm{e}^{-t^2}\, \mathrm{d}t. \tag{10}$$

derived in Ref. 7. (ω_{pl} denotes the electron plasma frequency.)

For charged radiators, however, the divergence at $t = 0$ should not appear. This problem has been dealt with for example in Refs. 2 and 13.

In this paper, we calculate the field-field autocorrelation function at a charged point:

$$\Gamma(t) = \langle \boldsymbol{E}(\boldsymbol{r}(t=0)) \boldsymbol{E}(\boldsymbol{r}(t)) \rangle$$

$$= \frac{N}{V} \int \mathrm{d}\boldsymbol{r} \int \mathrm{d}\boldsymbol{v} f(\boldsymbol{v}) [- \nabla\varphi(\boldsymbol{r})][- \nabla\varphi(\boldsymbol{r}(t))]\, g_1(\boldsymbol{r}).$$

Where $g(\boldsymbol{r})$ denotes the pair correlation function we will consider weakly coupled plasmas, i.e. the coupling parameter $\Gamma \ll 1$. Therefore we employ the Debye–Hückel limit of the pair correlation function $g_1(r)$ and the pair potential $\varphi(r)$ in order to include the screening of the microfields as well as pair correlations, see Ref. 14

$$g(r) = \exp\left(- \frac{Z_0 e \varphi(r)}{k_B T} \right), \qquad \varphi(r) = \frac{1}{4\pi\varepsilon_0} \frac{Ze}{r} \mathrm{e}^{-\kappa r}.$$

Z_0 is the charge of the radiator, Z that of the ionic perturbers, and κ is the screening parameter. Assuming straight path trajectories ($r(t) = |\boldsymbol{r} - \boldsymbol{v}t|$) for the passing ions, the formula for the autocorrelation function

$$\Gamma(t) = \frac{k_B T}{Z_0 e} n_i \int \mathrm{d}\boldsymbol{v} f(\boldsymbol{v}) \int \mathrm{d}\boldsymbol{r}\, g_1(r) \Delta\varphi(r(t))$$

can be simplified to a single integral over r.

Thus, the resulting field correlation function is finite at $t = 0$:

$$\Gamma(t=0) = \frac{k_B T n_i}{\varepsilon_0} \frac{Z}{Z_0}, \tag{11}$$

and is in very good agreement with the results of Stehle[2] who assumed hyperbolic trajectories (Fig. 1).

The equation for $\Omega(E)$

$$\frac{1}{2\pi\mathrm{i}} \int_0^\Omega \mathrm{d}s \int_{c-\mathrm{i}\infty}^{c+\mathrm{i}\infty} \mathrm{d}t\, \Gamma(t)\, \mathrm{e}^{st} = \int_0^E F^2 W(F)\, \mathrm{d}F$$

has been solved using a parameterization for $\Gamma(t)$ which is accurate at least to 3%. However, the difference in the line width between using a charged point or neutral point MMM is negligible.

Further, including Doppler broadening in Eq. (1), the average over the velocities of the radiators has to be carried out applying the Maxwell distribution function. Fine structure splitting will be

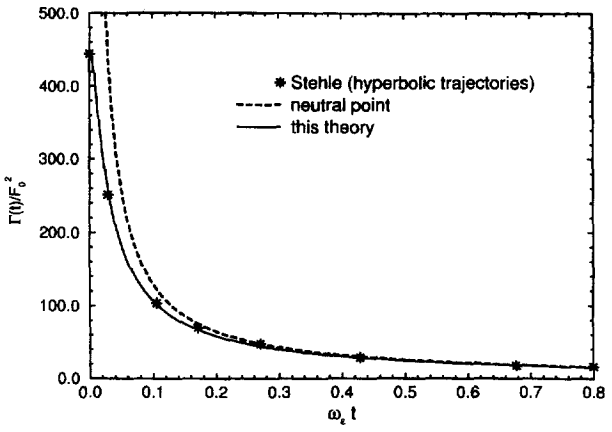

Fig. 1. Field-field autocorrelation function $\Gamma(t)$ at $n_e = 10^{15}\,\mathrm{cm}^{-3}$ and $T = 40\,000\,\mathrm{K}$ for hydrogen perturbers at a singly charged point (He^+).

accounted for by using the Pauli wave functions

$$u^{+}_{nlm} = \frac{1}{\sqrt{2l+1}} R_{nl} \begin{pmatrix} \sqrt{l+m+1/2}\, Y_{lm-1/2}(\theta,\phi) \\ -\sqrt{l-m+1/2}\; Y_{lm+1/2}(\theta,\phi) \end{pmatrix} \tag{12}$$

$$u^{-}_{nlm} = \frac{1}{\sqrt{2l+1}} R_{nl} \begin{pmatrix} \sqrt{l-m+1/2}\, Y_{lm-1/2}(\theta,\phi) \\ \sqrt{l+m+1/2}\, Y_{lm+1/2}(\theta,\phi) \end{pmatrix} \tag{13}$$

as the wave functions in Eq. (1). The corresponding unperturbed eigenvalues are given by

$$E = -\left(\frac{Z}{n}\right)^2 - \alpha^2 \left(\frac{Z}{n}\right)^4 \left(\frac{n}{j+\frac{1}{2}} - \frac{3}{4}\right), \tag{14}$$

where the quantum number j may take values between $\frac{1}{2}$ and $n - \frac{1}{2}$, n is the principal quantum number. Including the fine structure splitting, it is more complicate to carry out the average over the angles in Eq. (5) according to Eq. (7) compared to those evaluations given in the appendix of Ref. 11, where the usual spherical wave functions are applied.

Now, in principle, all the necessary formulae for the line profile are given. Only the concrete expressions for the electronic and the ionic self energy remain to evaluate. This will be done in the following two sections.

3. ELECTRONIC CONTRIBUTIONS TO THE SELF ENERGY

As it has been evaluated already for neutral radiators, the self energy within a second order Born approximation with respect to the perturber–radiator interaction is given by

$$\langle i|\Sigma(E_i^0 + \Delta\omega, \beta)|i\rangle = -\frac{1}{e^2} \int \frac{\mathrm{d}\boldsymbol{q}}{(2\pi)^3} V(q) \sum_{\alpha} |M_{i\alpha}^{(0)}(\boldsymbol{q})|^2 \int_{-\infty}^{\infty} \frac{\mathrm{d}\omega}{\pi} [1 + n_{\mathrm{B}}(\omega)] \times \frac{\operatorname{Im} \varepsilon^{-1}(\boldsymbol{q}, \omega + \mathrm{i}0)}{E_i^0 + \Delta\omega - E_\alpha(\beta) - (\omega + \mathrm{i}0)}. \tag{15}$$

This self energy depends on both the strength of the ionic microfield β and the detuning $\Delta\omega$ from the line center. The transition momentum q corresponds within a semiclassical picture, in principle, to an inverse impact parameter. $n_{\mathrm{B}}(\omega)$ is the Bose function

$$n_{\mathrm{B}}(\omega) = \frac{1}{\exp(-\omega/k_{\mathrm{B}}T) - 1}. \tag{16}$$

In principle, the α-sum has to be carried out over all bound and scattering states of the radiator. We restrict ourselves here to those states with principal quantum numbers n_α with

$$n_i - 1 \leq n_\alpha \leq n_i + 2,$$

where n_i is the principal quantum number of the considered state. Many particle effects are contained in the inverse dielectric function ε^{-1} which has been taken within the random-phase approximation. However, they do not play an important role for the plasma parameters considered here.

The matrix elements $M_{i\alpha}^{(0)}$ are given by

$$M_{i\alpha}^{(0)}(q) = \int \frac{dp}{(2\pi)^3} [\Psi_i^{ei}(p)]^* [Z_0 e \Psi_\alpha^{ei}(p) - e\Psi_\alpha^{ei}(p+q)], \tag{17}$$

where Ψ^{ei} are the radiator's wave functions.

For the matrix elements we use an expansion into spherical harmonics

$$e^{iqr} = 4\pi \sum_{l=0}^{\infty} \sum_{m=-l}^{l} i^l j_l(qr) Y_{lm}^*(\Omega_q) Y_{lm}(\Omega_r) \tag{18}$$

which corresponds to a quantum mechanical treatment of the perturbing electron. Here, we consider contributions up to $l = 2$ only. Calculating the width and the shift of the radiator's energy levels, one finds that the monopole-like $l = 0$ terms give the main contributions. These terms, however, one cannot find for the width and the shift of spectral lines since they are of the same magnitude for the upper and the lower energy level. Besides the $l = 1$ terms, contrary to the case of neutral radiators, also the quadrupole-like $l = 2$ terms become of importance. Therefore, the often used dipole-approximation should not be applied for the case of charged radiators.

If one would apply a second order Born approximation as in Eq. (15), however, the electronic contributions to width and shift of spectral lines would be overestimated. Therefore, strong collision contributions to shift and width have been treated systematically by a partial summation of the corresponding three-particle T-matrix as it has been done for hydrogen lines in Ref. 6.

Furthermore, of course, the corresponding wave functions and energy values in Eq. (15) change for charged radiators. Thus, the electronic contributions to the line width become much smaller than those for neutral radiators. The electronic width depends as Z^{-2} on the radiator's charge. Therefore, besides ion dynamics also the fine structure splitting may become important. For highly charged radiators, the same is true for the natural line width which grows as Z^4 with the charge of the radiator.

4. IONIC CONTRIBUTIONS TO THE SELF ENERGY

In order to calculate the line profiles according to Eq. (5), the time development operator for a constant ionic microfield strength has to be determined. In the static ion approximation, the Hamiltonian of a hydrogenic radiator including inhomogeneities of the ionic field as well as electron–ion and ion–ion interaction is given by

$$H(\beta) = H_0 + e_0 E_0 \beta z - \frac{5}{(32\pi)^{1/2}} \frac{e_0 E_0}{2R_0} B_\rho(\beta)(3z^2 - r^2), \tag{19}$$

where H_0 is the Hamiltonian of the isolated emitter, $\beta = E/E_0$ denotes normalized and $E_0 = e_0/R_0^2$ the normal Holtsmark field strength. R_0 is the mean distance defined by

$$\frac{4}{15}(2\pi)^{3/2} R_0^3 n_e = 1. \tag{20}$$

The function $B_\rho(\beta)$ includes the screening of the ionic microfield by the plasma electrons and has, therefore, to be considered as a generalization of the function $B(\beta)$ which has been introduced by Chandrasekhar and von Neumann.[15] In principle, it can be considered as a mean gradient of the microfield at a given field strength. This function depends on the screening parameter $\rho = R_0/D$, where D is the electronic Debye length.

In Eq. (19) a coordinate system with $\boldsymbol{E} \parallel \boldsymbol{E}_z$ has been chosen. From this Hamiltonian one finds the following contributions to the ionic self energy:

Besides the linear Stark effect

$$\sum_{ii}^{ls}(\beta) = \tfrac{3}{2} n^i (n_1^i - n_2^i)\,\beta E_0 \tag{21}$$

the quadratic Stark effect has been approximately accounted for by using

$$\sum_{ii}^{k}(\beta) = -\tfrac{1}{16}(n^i)^4 (17(n^i)^2 - 3(n_1^i - n_2^i)^2 - 9(m^i)^2 + 19)\beta^2 E_0^2. \tag{22}$$

Furthermore, the interaction between the radiator and the inhomogeneities of the ionic microfield has to be taken into account. The corresponding contributions due to the quadrupole interaction between the radiator and the ionic microfield are given by

$$\Sigma_{ii'}^{q}(\beta) = \begin{cases} \dfrac{\pi}{3} a_0^2 e^2 n_e (n^i)^2 \sqrt{n_1^i (n^i - n_1^i)\,(n_2^i + 1)\,(n^i - n_2^i - 1)}\, B_\rho(\beta): & \begin{matrix} n_1^i = n_1^{i'} - 1 \\ n_2^i = n_2^{i'} + 1 \end{matrix} \\ \dfrac{\pi}{3} a_0^2 e^2 n_e (n^i)^2 ((n^i)^2 - 1 - 6(n_1^i - n_2^i)^2) B_\rho(\beta): & i = i' \\ \dfrac{\pi}{3} a_0^2 e^2 n_e (n^i)^2 \sqrt{(n_1^i + 1)(n^i - n_1^i - 1) n_2^i (n^i - n_2^i)}\, B_\rho(\beta): & \begin{matrix} n_1^i = n_1^{i'} + 1 \\ n_2^i = n_2^{i'} - 1 \end{matrix} \end{cases} \tag{23}$$

In the Eqs. (18)–(23) parabolic quantum numbers with

$$n = n_1 + n_2 + |m| + 1 \tag{24}$$

according to Ref. 16 have been applied.

The function $B_\rho(\beta)$ which determines the ion-quadrupole contribution to the ionic self energy has been given for a neutral radiator in Ref. 11.

Here, this function has been calculated at a singly charged point ($Z_e = 1$) for single ($Z_p = 1$) and double ($Z_p = 2$) charged perturbers. The difference to the neutral radiator is here again the additional ion-ion interaction which has been described by the one body correlation function g_1. The essential expressions are given in the Appendix A. In Fig. 2, the relation between $B_\rho(\beta)$ and the ordinary function $B_0(\beta)$ is given as a function of the reduced field strength β for several values of the screening parameter ρ at a charged point for double charged perturbers. The corresponding ratio for singly charged perturbers is the same as it has been given in Fig. 2 of Ref. 11.

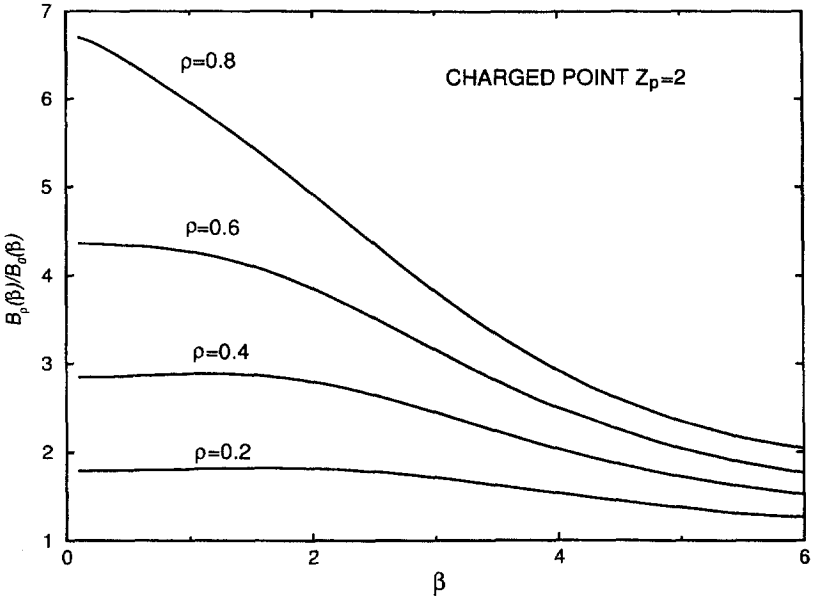

Fig. 2. Ratio of the field gradient functions $B_\rho(\beta)$ to that of the Holtsmark-case (see text).

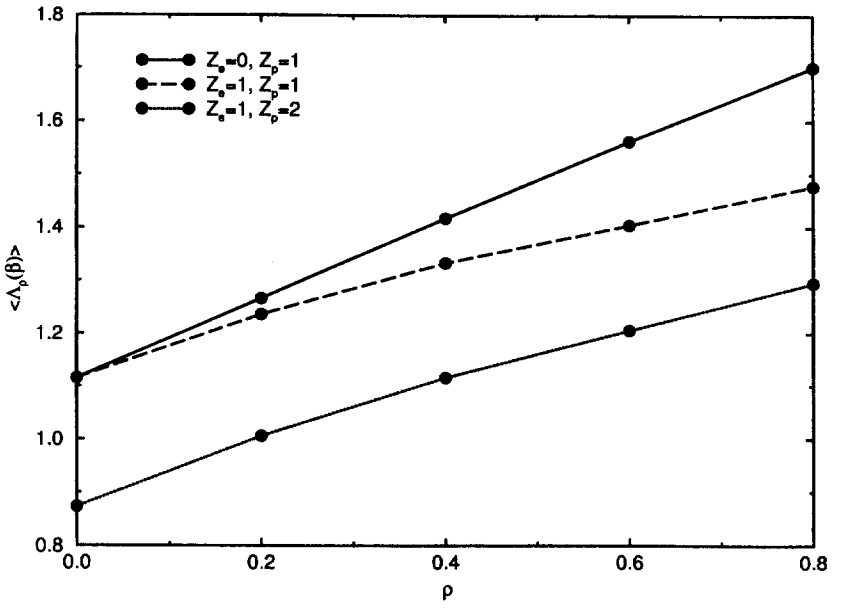

Fig. 3. Mean of $\Lambda_\rho(\beta)$ (explanation see text).

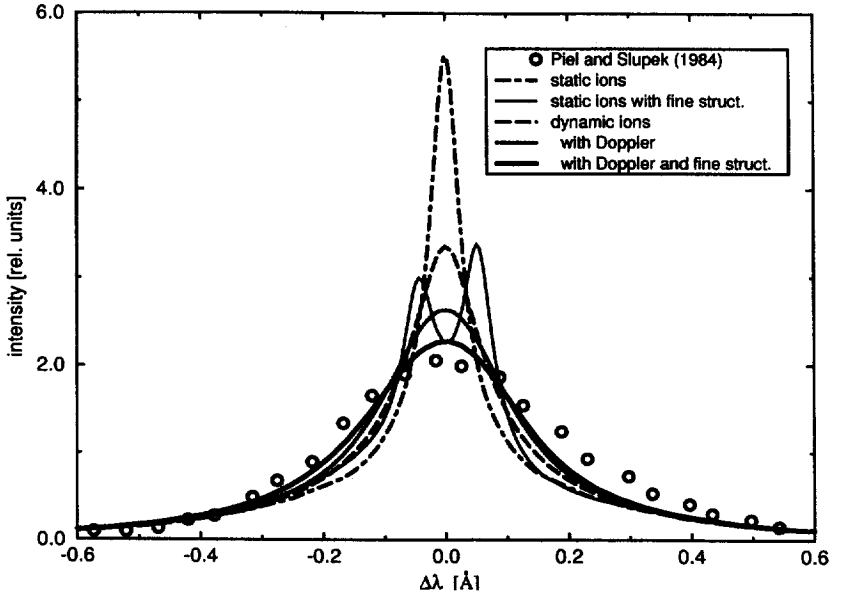

Fig. 4. Influence of various effects on the line profile of H_α at an electron density of $5.5 \times 10^{22}\,\mathrm{m}^{-3}$ and a temperature of $T = 44\,000$ K.

In Ref. 17 the function

$$\Lambda(\beta) = \frac{W_\rho(\beta) B(\beta)}{\beta} \tag{25}$$

has been introduced. Its generalisation within the Baranger/Mozer formalism has been given by one of the authors.[11] Whereas the dipole interaction between the radiator and the ionic microfield leads to terms proportional to β [see Eq. (19)], from the quadrupole interaction follow terms proportional to $B_\rho(\beta)$. Therefore, the mean value

$$\langle \Lambda_\rho \rangle = \int_0^\infty \frac{B_\rho(\beta)}{\beta} W_\rho(\beta)\, \mathrm{d}\beta \tag{26}$$

is a measure of the importance of the quadrupole interaction compared to the dipole term. It becomes obvious from Fig. 3 that the relative importance of the ion-quadrupole terms decreases with an increasing degree of the plasma ionization.

5. RESULTS

With the theory outlined in the previous sections, the profiles of some He II lines have been calculated. In Fig. 4 the influence of various effects on the line profile such as fine structure splitting, ion dynamics and Doppler broadening are investigated. Analogous to the corresponding experiment

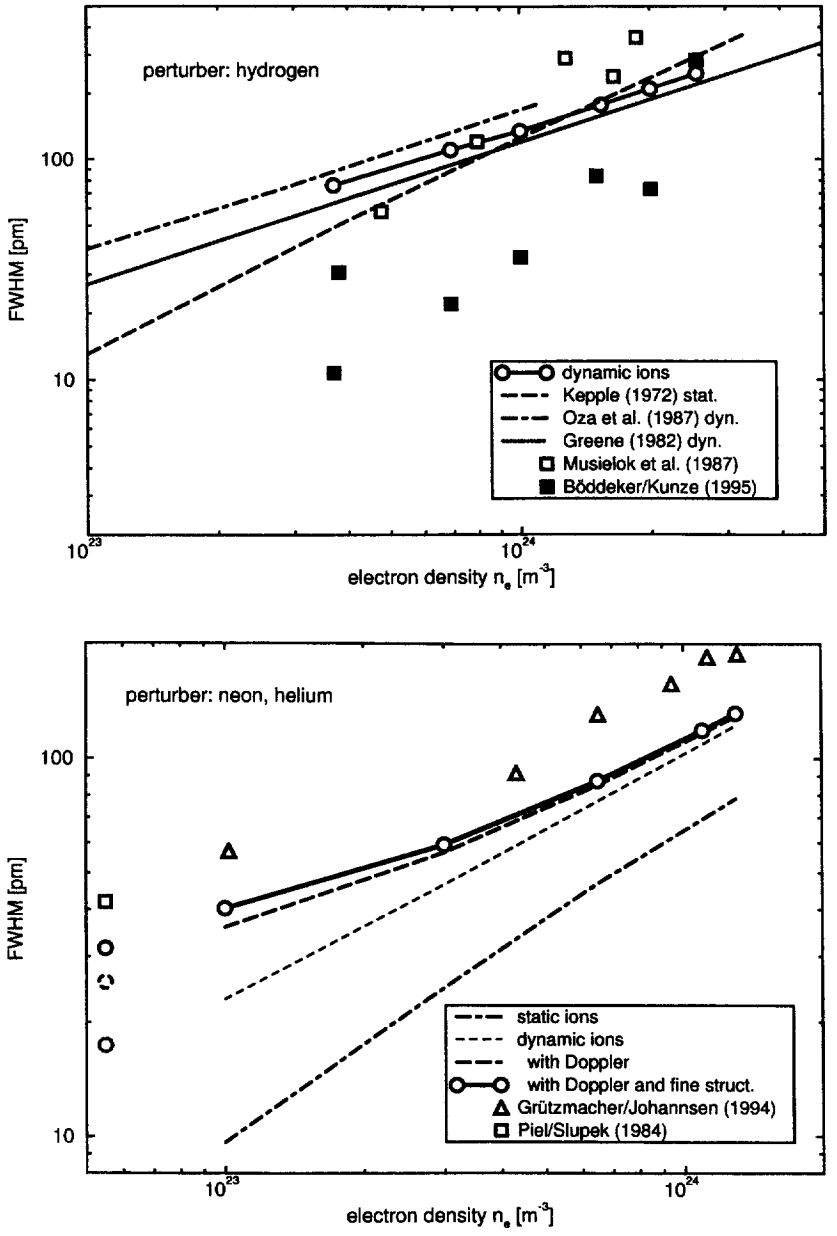

Fig. 5 (a) Width of the H_α-line compared to several experimental and theoretical results. The results of Greene and Oza have been taken from Refs. 19, 21 resp. and include ion dynamics whereas the values of Kepple[22] are for static ions. The experiments stem from Musielok et al[23] and Böddeker and Kunze.[24] (b) Same as (a), but the effects of fine structure and ion dynamics over a wide range of densities are shown. Density and temperature of the calculated results correspond to those of the experimental data.

by Piel and Slupek[1], an electron density of $5.5 \times 10^{22}\,m^{-3}$ and a temperature of 44 000 K have been chosen. As it has been already outlined in Ref. 1, there is a large discrepancy between the experimental and the theoretical line width assuming a static ionic microfield and neglecting further fine structure splitting as well as Doppler broadening. Taking into account the Doppler broadening only, the half width already increases considerably. The same effect can be found including only the fine structure splitting. Considering simultaneously the fine structure splitting, the effects due to ion dynamics and the Doppler broadening, one reaches a much better agreement between experimental and theoretical results.

There are a lot of experimental results for the width of the H_α line of He II. As can be seen in Fig. 5(a), the various experimental results differ clearly. Therefore, it is not possible to make statements about the quality of the various theories. Considering the experimental results for the half width of the H_α line which has been given recently by Grützmacher and Johannsen[18] [Fig. 5(b)], one finds that the density dependence of the half width agrees, at least qualitatively, with the theory. Despite of the inclusion of the fine structure splitting as well as ion dynamics, however, the theoretical half width remains too small compared to the experiment. This is presumably caused by the well-known underestimation of the ion dynamical effects within the applied model microfield method. The same is true for the half width of the P_α-line (Fig. 6). Our theoretical line width agree very well with that given by Greene [19] who used a relaxation theory in order to describe ion dynamical effects.

In the Figs. 7 and 8, the shift of the H_α and the P_α lines are compared to experimental results. It becomes obvious that the shift of the P_α line agrees excellently with the measured one, whereas the theoretical shift of the H_α line is much smaller than the corresponding experimental result. We do not know the reasons for this discrepancy. In theoretical evaluations as described in this paper, the relation between the shifts of H_α and P_α is given by the corresponding transition matrix elements. As it has to be expected, the relation between both shifts at a given electron density calculated by this paper is nearly the same as given by Griem. Obviously, within common theories it is impossible to reach a good agreement between experimental and theoretical shifts for both lines at the same time. Possibly, ion dynamical effects to the line shift which have not been included here are large enough to result in a remarkably red shift of the H_α line so that this discrepancy can be removed.

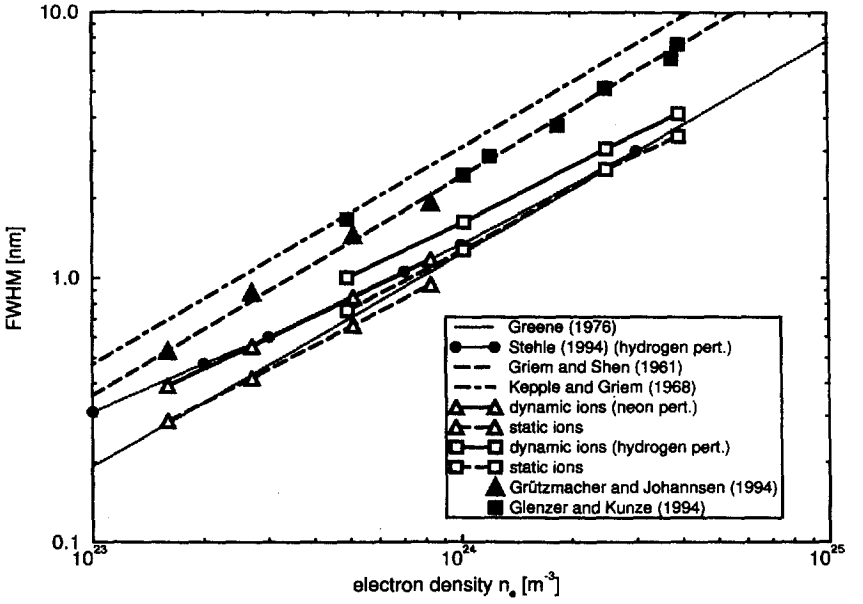

Fig. 6. Width of the P_α-line compared to several experimental and theoretical results: In Ref. 2 ion dynamics have been included applying the model microfield method. The results of Greene[25] are static ion results as well as those of Griem and Shen[26] and Kepple and Griem.[27] In Refs. 26, 27 the upper–lower interference terms are neglected.

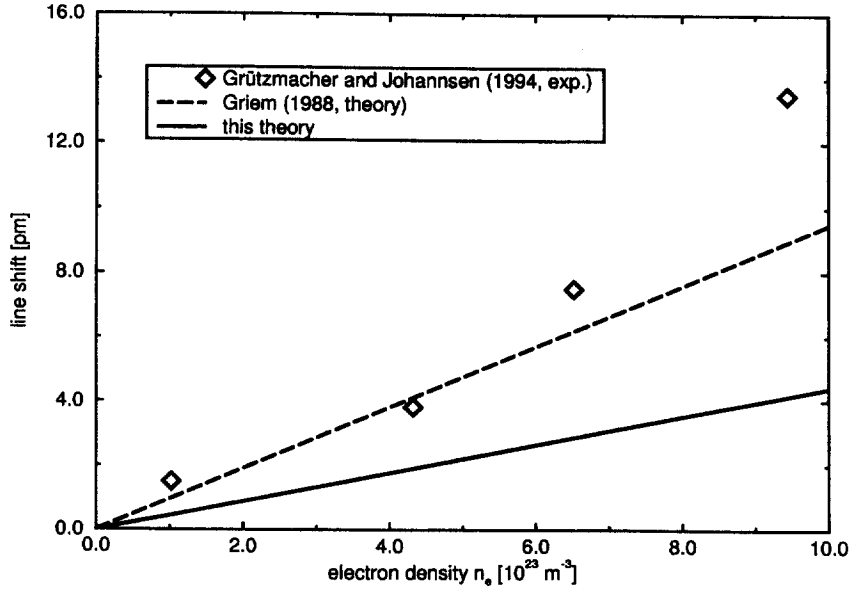

Fig. 7. Shift of the maximum of the H_α-line. The comparison has been made to theoretical results of Griem[28] and experimental values of Grützmacher and Johannsen.[18]

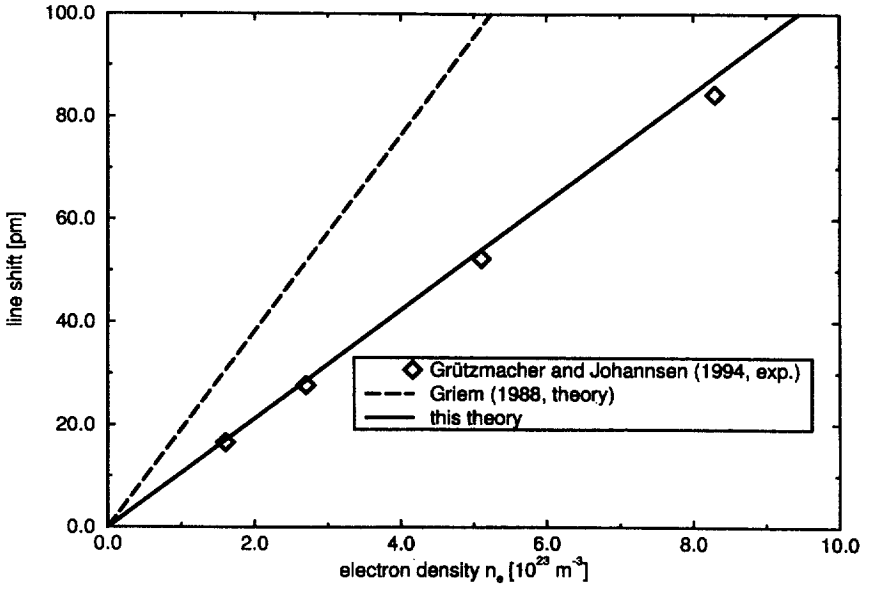

Fig. 8. Shift of the maximum of the P_α-line. The comparison has been made to Refs. 18, 28.

6. CONCLUSIONS

The many-particle approach to spectral line shapes developed for neutral radiators has been generalized to charged radiators. Within this approach, the perturbing electrons have been treated quantum-mechanically. Further, strong collision contributions have been included systematically by a partial summation of the corresponding three-particle T-matrix. Thus, no arbitrary parameters are necessary calculating widths as well as shifts of spectral lines.

Besides the electronic contributions to the line profile, the influence of the plasma ions have been included via the well known model microfield method. Thereby, not only the ionic contributions to the line width but also to its shift have been included. In order to deal with the interaction between

the radiator and the inhomogeneities of the ionic microfield, the corresponding expressions given in Ref. 11 for neutral radiators have been generalized for the case of charged radiators. Furthermore, fine structure effects have been included.

Applying the developed theory, the profiles of the H_α and P_α lines of He II have been calculated and compared to recent experimental results. The theoretical dependence of the width on the electron density for both lines agrees, at least qualitatively, with the experimental results. Nevertheless, it must be stated that the inclusion of fine structure splitting does not remove the discrepancies between the already published theoretical and experimental results. For low electron densities, however, the fine structure splitting plays an important role. The remaining discrepancies between theoretical and experimental line widths are presumably caused by the underestimation of ion dynamics within the applied model microfield method. The shift of the P_α line agrees excellently with experimental results. For the H_α line, however, large discrepancies between theoretical and experimental line shifts occur. The reason for these discrepancies are unclear. Within all the developed theories up to now, it is impossible to reach at the same time a good agreement with the experimental results for both, the H_α and the P_α lines since the theoretical line shift depends on the corresponding transition matrix elements.

Acknowledgements—This work has been supported by the Sonderforschungsbereich 198.

REFERENCES

1. Piel, A. and Slupek, J., *Zs. Naturforsch.*, 1984, **39a,** 1041.
2. Stehle, C., *Astron. & Astrophys. Suppl.*, 1994, **104,** 509.
3. Hitzschke, L., Röpke, G., Seifert, T. and Zimmermann, R., *J. Phys. B: At. Mol. Phys.*, 1986, **19,** 2443.
4. Hitzschke, L., Röpke, G., *Phys. Rev.*, 1988, **A37,** 4991.
5. Günter, S., Hitzschke, L. and Röpke, G., *Phys. Rev.*, 1991, **A44,** 6834.
6. Günter, S., *Phys. Rev.*, 1993, **E48,** 500.
7. Brissaud, A., et al, *J. Phys. B: At. Mol Phys.*, 1976, **9,** 1129.
8. Brissaud, A., Goldbach, C., Leorat, L. and Mazure, A., *J. Phys. B: At. Mol. Phys.*, 1976, **9,** 1147.
9. Seidel, J., *Zs. Naturforsch.*, 1977, **32a,** 1195.
10. Seidel, J., *Z. Naturforsch.*, 1980, **35a,** 679.
11. Halenka, J., *Z. Phys. D*, 1990, **16,** 1.
12. Günter, S. and Könies, A., *Phys. Rev. E*, 1997, **55,** 907.
13. Boercker, D., Iglesias, C. and Dufty, J., *Phys. Rev.*, 1987, **A36,** 2254.
14. Iglesias, C., Lebowitz, J. and Gowan, D. M., *Phys. Rev.*, 1983, **A28,** 1667.
15. Chandrasekhar, S. and von Neumann, J., *Astrophys. J.*, 1943, **97,** 1.
16. Landau, L. and Lifschitz, E., Lehrbuch der theoretischen Physik. Band 3 Akademie Verlag, Berlin, 1986.
17. Demura, A. and Sholin, G., *J. Quant. Spectrosc. Rad. Transfer*, 1975, **15,** 881.
18. Grützmacher, K. and Johannsen, U., Frühjahrstagung der DPG, Greifswald, 1993 (unpublished).
19. Greene, R. L., *J. Phys. B: At. Mol. Phys.*, 1982, **15,** 1831.
20. Oks, E. A., Derevianko, A. and Ispolatov, Y., *J. Quant. Spectrosc. Rad. Transfer*, 1995, **54,** 307.
21. Oza, D., Greene, R. and Kelleher, D., *Phys. Rev.*, 1987, **A37,** 531.
22. Kepple, P., *Phys. Rev.*, 1972, **A6,** 1.
23. Musielok, J., Bottcher, F., Griem, H. and Kunze, H.-J., *Phys. Rev.*, 1987, **A36,** 5683.
24. Böddeker, S. and Kunze, H.-J., Frühjahrstagung der DPG, Innsbruck, 1995 (unpublished).
25. Greene, R. L., *Phys. Rev.*, 1976, **A14,** 1447.
26. Griem, H. and Shen, K., *Phys. Rev.*, 1961, **122,** 1490.
27. Kepple, P. and Griem, H., *Phys. Rev.*, 1968, **173,** 317.
28. Griem, H., *Phys. Rev.*, 1988, **A38,** 2943.
29. Baranger, M. and Mozer, B., *Phys. Rev.*, 1959, **115,** 521.
30. Mozer, B. and Baranger, M., *Phys. Rev.*, 1960, **118,** 626.

APPENDIX A

The general formalism for calculating the function $B_\rho(\beta)$, as described in Ref. 11, remains unchanged. Using the same designations the as in Ref. 11, we can express $B_\rho(\beta)$ by auxiliary functions $\Psi(v)$ as follows:

$$B_\rho(\beta) = \int_0^\infty dx\, x^2[\Psi_1^{(1)}(v) + \Psi_2^{(1)}(v)] \exp\{-x^{3/2}[\Psi_1^{(0)}(v) - \Psi_2^{(0)}(v)]\} j_2(\beta x) \Big/ \int_0^\infty dx\, x^2 \exp\{-x^{3/2}[\Psi_1^{(0)}(v) - \Psi_2^{(0)}(v)]\} j_0(\beta x), \tag{A1}$$

where j_l is the spherical Bessel function of order l, and $v = \rho x^{1/2}$. In order to calculate the auxiliary functions Ψ we use the same approximation for the correlation functions as in Refs. 29 and 30. The one-body correlation function is then given by

$$g_1 = \exp\{ - Z_p(4\pi D^2 n_e)^{-1}|\boldsymbol{R}_1|^{-1}\exp(- R_D|\boldsymbol{R}_1|/D)\}, \tag{A2}$$

and the two-body function reads

$$g_2 = - Z_p^2(4\pi D^2 n_e)^{-1}|\boldsymbol{R}_1 - \boldsymbol{R}_2|^{-1}\exp(- R_D|\boldsymbol{R}_1 - \boldsymbol{R}_2|/D), \tag{A3}$$

where $R_D = (1 + Z_p)^{1/2}$ and $D = \sqrt{(e_0 k_B T)/(e^2 n_e)}$.

Then, the auxiliary functions can be expressed as

$$\Psi_1^{(0)} = 15(8\pi)^{-1/2}\int_0^\infty dy \exp\left\{ - \frac{2(2\pi)^{1/2}}{15} Z_p R_D \rho^3 \frac{\exp(- u)}{u}\right\}[1 - j_0(\varepsilon)]y^2, \tag{A4}$$

$$\begin{aligned}\Psi_2^{(0)} &= 15(8\pi)^{-1/2} R_D v^3/n_e^2 \int_{y_1=0}^\infty y_1^2\, dy_1 \int_{y_2=0}^{y_1} y_2^2\, dy_2 \sum_{l=0}^\infty (- 1)^l(2l + 1)[j_l(\varepsilon_1) - \delta_{l,0}] \\ &\quad \times [j_l(\varepsilon_2) - \delta_{l,0}] f_l^>(u_1) f_l^<(u_2),\end{aligned} \tag{A5}$$

$$\Psi_1^{(1)} = 6\int_0^\infty y_1^2 \gamma(v, y_1) j_2(\varepsilon_1)\, dy_1, \tag{A6}$$

and finally

$$\begin{aligned}\Psi_2^{(1)} &= 12 R_D Z_p v^3 \int_{y_1=0}^\infty y_1^2\, dy_1 \int_{y_2=0}^{y_1} y_2^2\, dy_2 \gamma(v, y_1) \\ &\quad \times \left[j_2(\varepsilon_1) - \sum_{l=0}^\infty (- 1)^l(2l + 1)\left\{\left[\frac{3}{2} l(l - 1)\varepsilon_1^{-2} - 1\right] j_l(\varepsilon_1) + 3\varepsilon_1^{-1} j_{l+1}(\varepsilon_1)\right\} j_l(\varepsilon_2)\right] f_l^>(u_1) f_l^<(u_2).\end{aligned} \tag{A7}$$

with

$$\varepsilon(v, y) = Z_p y^{-2}(1 + vy)\exp(- vy), \tag{A8}$$

$$\gamma(v, y) = y^{-3}[1 + vy + (vy)^2/3]\exp(- vy), \tag{A9}$$

$$u = R_D vy, \tag{A10}$$

$$y = (ke_0)^{-1/2} R. \tag{A11}$$